Quantum Chemistry Study on the Interaction of the Exogenous Ligands and the Catalytic Zinc Ion in Matrix Metalloproteinases

Feng Cheng,[†] Ruihao Zhang,[†] Xiaomin Luo,[†] Jianhua Shen,[†] Xin Li,[†] Jiande Gu,[†] Weiliang Zhu,[†] Jingkang Shen,[†] Irit Sagi,[‡] Ruyun Ji,[†] Kaixian Chen,[†] and Hualiang Jiang*,[†]

Center for Drug Discovery and Design, State Key Laboratory of Drug Research, Shanghai Institute of Materia Medica, Shanghai Institutes of Biological Sciences, Chinese Academy of Sciences, 294 Taiyuan Road, Shanghai 200031, P. R. China, and Department of Structural Biology, The Weizmann Institute of Science, Rehovot 76100, Israel

Six zinc complexes, $Zn(imidazole)_3X$ (where X = water, CH_3S^-, hydroxamate, formylhydroxylamine, hypophosphite, and acetate), have been calculated with the density functional theory (DFT) method B3LYP/ 6-31G* to probe the interaction between the exogenous ligands and the catalytic zinc ion in matrix metalloproteinases (MMPs). According to our calculation, their interaction modes can be divided into three classes. The structural features of these complexes are in agreement with the X-ray data in the Cambridge Structural Database and the Protein Data Bank. The atomic charge analyses proved that the catalytic water molecule in the active site of MMPs can be activated after coordinating with the zinc ion and thus acts as a good nucleophile to attack and degrade the substrate of MMPs. The geometric parameters of these complexes, the charge transfers from the exogenous ligands to the Zn(II), and the calculated relative binding free energy characterize well the binding ability of these ligands with the zinc ion. The inhibitory activities of the MMP inhibitors, which contain the same substituents and different zinc binding groups (ZBGs), correlate well with the binding free energies predicted by the DFT calculation with correlation coefficients of 0.969 for matrilysin and 0.939 for human fibroblast collagenase (HFC). This gives a possible good strategy for predicting the inhibitory activity for the newly designed inhibitors of MMPs; those potential inhibitors that would exhibit strong binding ability of ZBGs to Zn(II) using this paradigm would therefore be expected to have greater inhibitory activity.

Introduction

Matrix metalloproteinases (MMPs) are a family of zinc proteinases that degrade and remodel the extracelluar matrix (ECM).[1,2] The excess synthesis and expression of these proteins results in the accelerated matrix degradation associated with a series of diseases such as cancer, arthritis, and multiple sclerosis.[3,4] Therefore, developing MMP inhibitors may provide a new treatment for these diseases, especially for cancer.[5,6]

Experiments have shown that the catalytic zinc ion in the active site of MMPs is directly involved in the ECM degradation process.[7,8] In the latent form of MMPs, the zinc ion is bound by three histidine residues in a conserved zinc binding motif, HEXXHXXGXXH, and the sulfhydryl group of Cys73 in the propeptide, which blocks the active site of MMPs. Upon activation, cleavage of the propeptide results in the dissociation of Cys73 and the active site being accessible for substrate binding.[9] Consequently, the catalytic zinc ion coordinates and degrades the substrate. Because zinc ion plays an important role in the substrate degradation process, one of the key questions in the design of MMP inhibitors is how to find the best zinc binding groups (ZBG) to compete with substrate to coordinate zinc ion. Structure-based drug design (SBDD) has been successfully applied in new drug design.[10–12] However, the normal

SBDD methods such as DOCK,[11,13,14] which were developed on the basis of the empirical force fields, cannot be employed directly in designing ZBGs of MMPs and other metalloproteinases, because it is concerned with coordination bond making and breaking. Thus computational methods developed based on the first principle quantum mechanics, such as quantum chemistry ab initio methods[15] or density-functional theory (DFT) methods,[16] have to be used in studying the binding properties and mechanism of a ZBG with Zn(II), and in designing the ZBGs.

In our previous paper,[17] we studied the catalytic active site of natural human gelatinase B (MMP-9) in its latent and activated states employing X-ray absorption spectroscopy (XAS) combined with the density functional theory (DFT) calculations for three model structures of MMPs. The results demonstrate the molecular rearrangement and conformational changes that occur upon activation in human gelatinase B at the zinc site. In this paper, we report in detail on the theoretical study of the coordination properties of six general ZBGs of MMP substrates and inhibitors. In addition, this paper provides a new strategy for predicting the binding ability of ZBGs, which may be used in designing new MMP inhibitors.

Models and Computational Methods

The typical zinc coordination sphere in MMPs consists of three histidine (His) residues and one exogenous ligand. These histidine residues were modeled by imidazole, and the coordination sphere can be represented by $Zn(imidazole)_3X$, where X is

---

* To whom correspondence should be addressed. Phone: +86-21-64311833 ext 222. Fax: +86-21-64370269. E-mail: jiang@iris3.simm.ac.cn or hljiang@mail.shcnc.ac.cn.
† Shanghai Institutes of Biological Sciences.
‡ The Weizmann Institute of Science.

Quantum Chemistry Study on the Interaction

J. Phys. Chem. B, Vol. 106, No. 17, 2002 **4553**
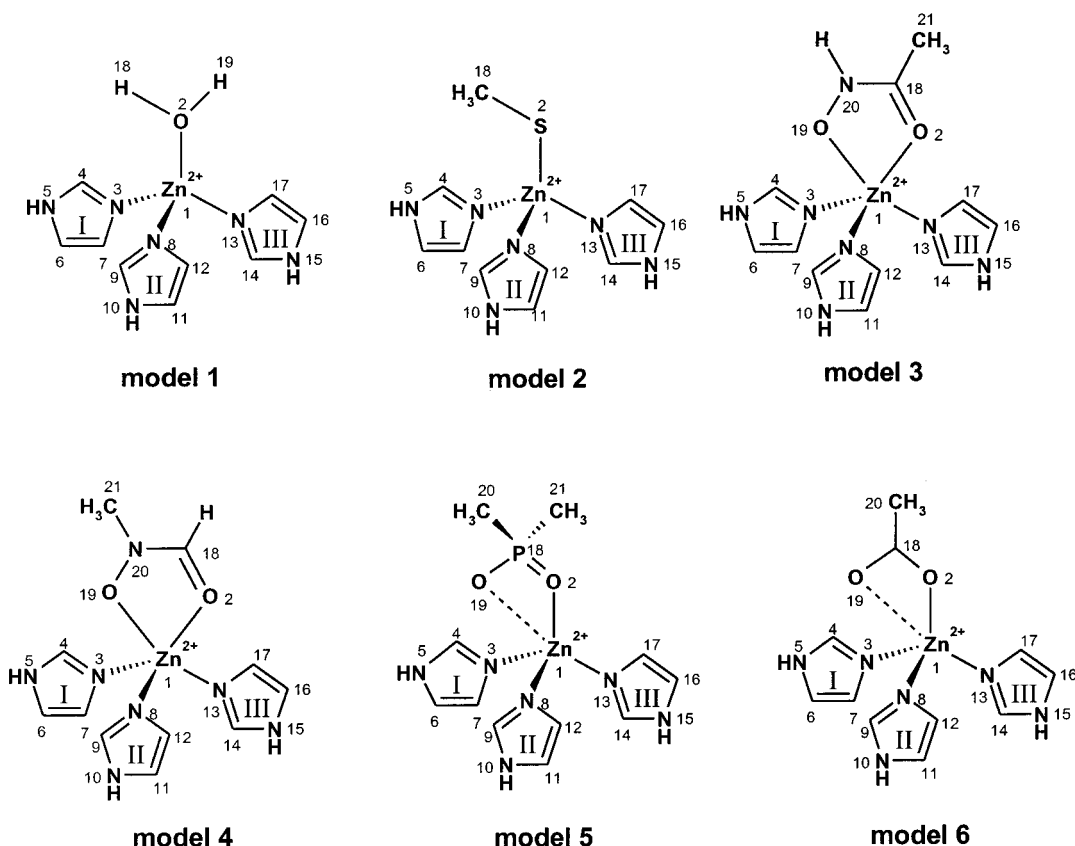
Figure 1. Schematic presentation of the six models of zinc complexes. The symbols and numbers designate the different atoms.

the exogenous ligand. The ligand may be a substrate, the ZBG of an inhibitor, or a water molecule. In the present paper, six ligands were investigated to mimic catalytic water, cysteine, and some typical ZBGs of MMP inhibitors. These ligands are water (model **1**), CH_3S^- (model **2**), hydroxamate (model **3**), formylhydroxylamine (model **4**), hypophosphite (model **5**), and acetate (model **6**) (Figure 1).

The quantum chemistry calculation method B3LYP,[18] a density-functional theory (DFT) type of calculation approach based on a hybrid functional, has shown to be the most accurate density functional method, and it gives as good or better geometries and energies as those from correlated ab initio methods for the first-row transition metal complexes.[19] Its computational speed is, on the other hand, much faster than that of the MP2 (Möller–Plesset second-order perturbation).[20] We therefore selected B3LYP to optimize the structures of the model molecules at the basis level of 6-31G*. Frequency calculation was then carried out to verify the reasonability of the optimized structures and to determine thermal parameters such as thermal energy, E_{therm}, and entropies, S. It is well-known that the treatment of anionic species needs the inclusion of diffused orbitals. Therefore, to evaluate the internal energy, E_t, more accurately, single-point energy calculations were performed on the optimized geometries of 6-31G* using the basis set 6-31+G**, which includes diffused orbitals.

All quantum chemistry calculations were carried out with the Gaussian 98 program[21] on a Power-Challenge R10000 supercomputer. The molecular modeling was performed on an SGI workstation with the SYBYL 6.6 software package.[22]

Results and Discussion

The Structural Characteristics of the Complexes. Figure 2 depicts the optimized structures by B3LYP/6-31G* of the six

models. The frequency calculation results of these optimized structures showed that no imaginary frequency exists, indicating that these optimized structures are true minimum energy structures. Their geometric parameters are summarized in Table 1.

Four-Coordination Complexes. Water and CH_3S^- coordinate with Zn(II) in a monodentate model to form four-coordination complexes, because these two ligands only have one heteroatom to coordinate with the Zn(II). A four-coordination model may give either tetrahedral or square-planar coordination geometry. The electron configuration of the Zn(II) ion is $3d^{10}$. It coordinates with the ligands and three imidazole molecules using its 4s and 4p orbitals in sp^3 hybrid orbitals. According to the valence shell electron pair repulsion (VSEPR) theory, tetrahedral configurations are favored for the Zn(II) four-coordination complexes, as in $[ZnCl_4]^{2-}$. This also can be observed from the optimized structures and geometry parameters of the two models. As shown in Figure 2, both of model **1** and model **2** adopt asymmetric and little distorted tetrahedral structure. The O–Zn–N bond angles in model **1** are 110.0°, 100.4°, and 102.1°, respectively, and the three bond angles of S–Zn–N in model **2** are 109.4°, 109.2°, and 120.3°, which are close to that of the standard tetrahedral configuration (109.5°).

Five-Coordination Complexes. The coordination modes of hydroxamate and formylhydroxylamine with Zn(II) are more complex than those of water and CH_3S^-. They have two oxygen atoms and may bond to Zn(II) in two different ways: monodentate and bidentate configurations that result in four- and five-fold coordinations with the zinc ion, respectively. The two ligands bond with Zn(II) using the latter way, because the geometries of the two complexes are close to standard five-fold coordination configurations. As shown in Table 1, the bond angles of 2–1–3 and 2–1–8 in these two complexes are 120.9°
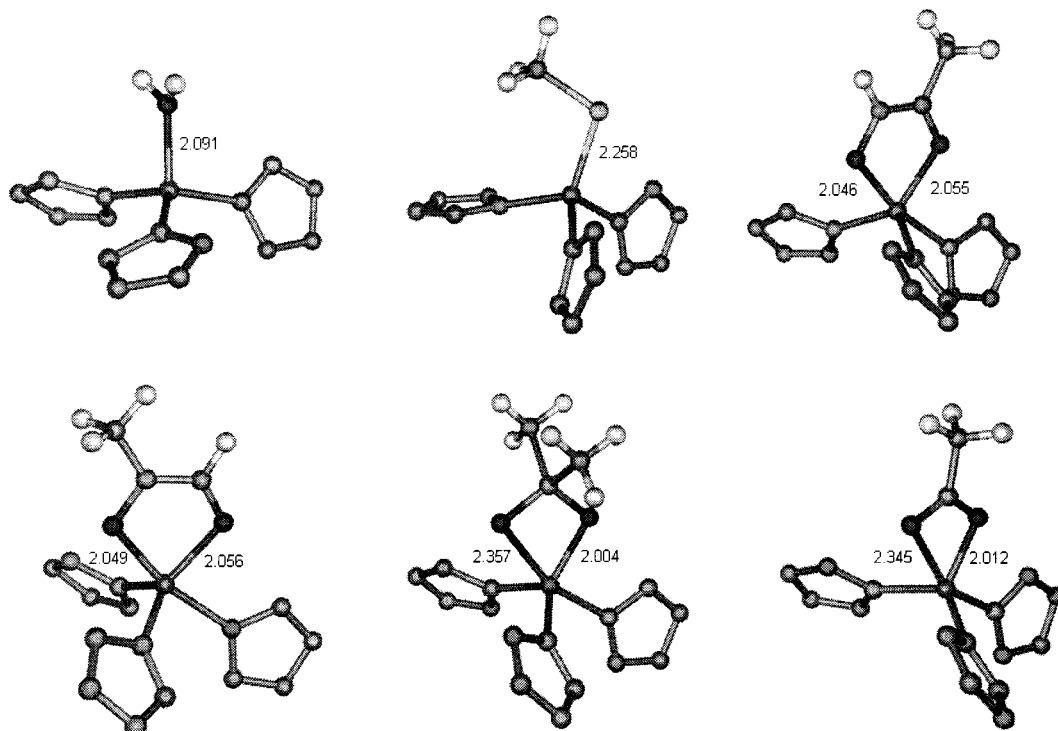
Figure 2. The optimized structures of the six zinc complexes. Hydrogens of imidazole rings are not displayed for clarity. Some key bond lengths (in Å) are displayed.

and 121.0°, respectively. The bond angles of 2—1—13 and 2—1—19 for model **3** are 86.2° and 80.8° and those for model **4** are 85.7° and 80.4°. These geometric parameters are very close to the trigonal bipyramidal geometry, a typical configuration of a five-coordination complex. In addition, the bond lengths of the two Zn—O bonds are almost equal, 2.055 and 2.046 Å in model **5** and 2.056 and 2.049 Å in model **4**, which also indicates that the two oxygens may coordinate with the Zn(II) equally. The five-fold coordination configuration of Zn(II) is ubiquitous in enzyme—inhibitor complexes in the Protein Data Bank (PDB).[5,23,24]

Complexes between Four- and Five-Fold Coordinations. Like hydroxamate and formylhydroxylamine, the acetate group also can coordinate to a zinc ion in two possible modes. In a way different from Ryde's calculation,[19] we optimized the geometry of model **6** without any constraint (Ryde optimized this structure in monodentate and bidentate geometries by constraining the Zn1—O2—C18 angle as 120° and 90°, respectively). The optimized geometry of model **6** gives the bond angle of Zn1—O2—C18 as 96.8°, which is between the region of Ryde's constraint of 120° and 90° for monodentate and bidentate configurations. This also can be seen from the structure parameters listed in Table 1. The bond angles of O2—Zn1—N3, O2—Zn1—N8, and O2—Zn1—N13 are 119.5°, 116.2°, and 93.7°, which also indicate that the geometry of model **6** is between the regular trigonal bipyramidal (120°, 120°, and 90°, respectively) and tetrahedral (120°, 120°, and 120°, respectively) structures. In addition, the Zn—O distances (Zn1—O2 and Zn1—O19) are, respectively, 2.012 and 2.345 Å, which are very close to those of the carboxylate complexes of zinc in the Cambridge Crystal Database,[19,25] 2.16 ± 0.1 and 2.40 ± 0.14 Å, respectively; and these two kinds of distances are more close to those of the zinc—carboxylate complexed proteins, which are 2.08 ± 0.06 and 2.31 ± 0.09 Å.[25] On the other hand, the geometry of the carboxylate group varies greatly after coordination with Zn²⁺. As can be seen from Tables 1 and 2, in the complex, the

bond length of O2—C18 lengthened about 0.03 Å; bond C18—O19 only lengthened 0.005 Å; however, this bond swung toward Zn(II), which diminishes the bond angle of O2—C18—O19 from 129.8° in its free state to 120.3°. All of these further indicate that O2 coordinates with Zn²⁺ directly and that O19 does so only partially. Because of this, we can regard bond Zn1—O19 as a partial coordination bond and the coordination number of model **6** could be between four and five. The same coordination can be observed in hypophosphite. We therefore represent acetate and hypophosphite as half-bidentate ligands.

Charge Population Analysis. *Group Charges.* Table 2 presents the atomic charges and group charges of the six complexes. The group charge was calculated by the summation over the atomic charges of all of the atoms that compose the group. As shown in Table 2, the group charges of the six ligands in free states are 0.0, −1.0, −1.0, −1.0, −1.0, and −1.0 Q/e, while those of the ligands in complexes are 0.165, −0.366, −0.477, −0.482, −0.471, and −0.531 Q/e. It is seen that the group charges of the ligands all increase in the complexes coordinating with Zn(II), which indicates that electron transfer from ligands to Zn(II) has occurred and the coordination bonds have formed.

Atomic Charges. The atomic charge calculations can give a feature for the relocation of the electron density of the ligands. The monodentate ligands (water and CH₃S⁻) coordinate to Zn-(II) with a single coordinated atom. As shown in Table 2, the atomic charge of the zinc-bound atom S2 in CH₃S⁻ increases in model **2** (from −0.785 to −0.333 Q/e). However, the atomic charge of O2 of water in model **1** is more negative (from −0.774 to −0.789 Q/e). In other words, the oxygen atom of water in the complex does not lose an electron but keeps hold of its electrons. Where does the electron come from? We investigated the neighboring atoms and found that the atomic charges of the two hydrogen atoms in water (H18 and H19) increase remarkably (from 0.387 to 0.478 Q/e). Accordingly, we can

TABLE 1: Geometric Parameters of the Optimized Complexes and Free Ligands

	model **1**	model **2**	model **3**	model **4**	model **5**	model **6**
			Bond Length (Å)			
1−2	2.091	2.258	2.055	2.056	2.004	2.012
1⋯19			2.046	2.049	2.357	2.345
2−18	0.973	1.848	1.277	1.273	1.566	1.286
2−19	0.973					
18−19					1.536	1.261
18−20			1.321	1.317	1.821	1.509
18−21			1.501		1.821	
19−20			1.353	1.355		
20−21				1.450		
			Bond Angles (deg)			
2−1−3	110.0	109.4	120.9	121.0	119.4	116.5
2−1−8	100.4	109.2	120.9	121.0	119.4	116.2
2−1−13	102.1	120.3	86.2	85.7	91.1	93.4
2−1−19			80.8	80.4	69.5	61.9
1−2−18	122.0	104.5	110.9	110.0	97.7	96.8
18−2−19	106.7					
2−18−19					107.6	120.3
2−18−20			119.5	121.9	109.3	118.7
2−18−21			121.4		109.3	
18−20−19			121.5	119.0		
20−18−21			119.1		106.5	
18−20−21				125.4		
19−20−21				115.6		
2−18−20−19			0.0	0.0		180.0
19−20−18−21			180.0			
2−18−20−21				180.0		

	water	CH₃S⁻	hydroxamate	formylhydroxylamine	hypophosphite	acetate
			Bond Length (Å)			
2−18	0.969	1.817	1.253	1.246	1.517	1.257
2−19	0.969					
18−19					1.517	1.256
18−20			1.343	1.347	1.868	1.576
18−21			1.554		1.868	
19−20			1.333	1.337		
20−21				1.448		
			Bond Angles (deg)			
18−2−19	103.7					
2−18−19					109.5	129.8
2−18−20			127.6	128.4	107.9	115.1
2−18−21			119.9		107.9	
18−20−19			129.4	126.3		
20−18−21			112.5		100.8	
18−20−21				120.1		
19−20−21				113.5		
2−18−20−19			0.0	0.0		
19−20−18−21			180.0			
2−18−20−21				180.0		

deduce that the two hydrogen atoms transfer a greater amount of an electron to the oxygen atom than the oxygen atom transfers to Zn(II).

The atomic charge distributions can well explain why the MMPs are active only when the catalytic water molecule coordinates to Zn(II). Upon coordination to Zn(II), the negative charge of the oxygen atom in water increases. On the other hand, the atomic charges of the hydrogen atoms in water increase remarkably, which may lead to one of them departing and the water may alter into hydroxyl. These two factors make the catalytic water like a nucleophile to attack the substrate more effectively. Additionally, the water molecule is small; thus, the coordination sphere of zinc can accept more than one exogenous ligand, which may be a substrate or another water.[26] All of these demonstrated that water is an appropriate ligand that can be catalyzed by MMPs to hydrolyze substrates.

For the bidentate ligands (hydroxamate and formylhydroxylamine) and half-bidentate ligands (acetate and hypophosphite), the atomic charge change is more complex than that of the monodentate ligands. As shown in Table 2, the atomic charges of the coordinated atoms, O2 (from −0.640 to −0.600 Q/e) and O19 (from −0.639 to −0.579 Q/e) in acetate and O19 in hydroxamate (from −0.670 to −0.585 Q/e) and formylhydroxylamine (from −0.686 to −0.607 Q/e), increase. In contrast, the atomic charges of O2 (from −0.677 to −0.724 Q/e) and O19 (from −0.677 to −0.680 Q/e) in hypophosphite and O2 in hydroxamate (from −0.624 to −0.632 Q/e) and formylhydroxylamine (from −0.578 to −0.588 Q/e) decrease. This indicates that there is no general rule to predict the atomic charges for the coordinated atoms. However, group charges (Table 2) demonstrate that an electron transfers from the ligands to Zn(II) in the complexes, suggesting that an electron moves from the coordinated atoms to Zn(II) and the electron transfers synchronously from other parts of the ligands to the coordinated atoms.

Thermodynamic Parameters. Table 3 presents the theoretical results of the calculated internal energies (E_t), thermal energies (E_{therm}), and entropies (S) of all complexes and free

TABLE 2: The Charges (Q/e) of the Optimized Complexes and Free Ligands

	model **1**	model **2**	model **3**	model **4**	model **5**	model **6**
			Atomic Charges			
1	0.989	0.748	0.958	0.958	0.901	0.938
2	−0.789	−0.333	−0.632	−0.588	−0.724	−0.600
18	0.477	−0.566	0.615	0.322	1.115	0.616
19	0.478		−0.585	−0.607	−0.680	−0.579
20			−0.247	−0.005	−0.661	−0.523
21			−0.533	−0.311	−0.661	
			Total Atomic Charges			
Zn^{2+}	0.989	0.748	0.958	0.958	0.901	0.938
water	0.165					
CH_3S^-		−0.366				
hydroxamate			−0.477			
formylhydroxylamine				−0.482		
hypophosphite					−0.471	
acetate						−0.531

	water	CH_3S^-	hydroxamate	formylhydroxylamine	hypophosphite	acetate
			Atomic Charges			
2	−0.774	−0.785	−0.624	−0.578	−0.677	−0.640
18	0.387	−0.480	0.523	0.262	0.914	0.521
19	0.387		−0.670	−0.686	−0.677	−0.639
20			−0.242	0.010	−0.622	−0.502
21			−0.545	−0.271	−0.622	

TABLE 3: Thermodynamic Parameters of Six Complexes, Free Ligands, and Five Reactions[a]

	water	CH_3S^-	hydroxamate	formylhyd roxylamine	hypophosphite	acetate
E_t (hartree)[b]	−76.434	−438.134	−283.816	−283.811	−571.762	−228.543
	(−76.409)	(−438.110)	(−283.759)	(−283.760)	(−571.719)	(−228.498)
E_{therm} (kcal/mol)	15.04	24.584	43.034	43.922	55.975	33.497
S (cal/(mol K))	41.254	58.124	70.562	71.751	78.163	64.088

	model **1**	model **2**	model **3**	model **4**	model **5**	model **6**
E_t (hartree)	−2533.936	−2895.923	−2741.631	−2741.620	−3029.547	−2686.332
	(−2533.850)	(−2895.837)	(−2741.538)	(−2741.530)	(−3029.455)	(−2686.246)
E_{therm} (kcal/mol)	166.490	176.055	195.821	195.951	207.369	184.087
S (cal/(mol K))	148.139	160.700	161.348	160.708	169.227	155.894

	reaction 1	reaction 2	reaction 3	reaction 4	reaction5
ΔE_t (kcal/mol)	−180.10	−196.41	−192.65	−177.59	−180.10
	(−179.47)	(−212.10)	(−206.45)	(−185.12)	(−192.65)
ΔE_{therm} (kcal/mol)	0.04	1.36	0.6	−0.04	0.23
ΔH (kcal/mol)	−180.06	−195.05	−192.05	−177.63	−179.87
	(−179.43)	(−210.74)	(−205.85)	(−185.16)	(−192.42)
ΔS (cal/(mol K))	0.952	−10.8	−12.63	−10.52	−8.78
ΔG (kcal/mol)	−180.34	−193.19	−188.89	−174.45	−177.48
	(−179.71)	(−207.52)	(−202.09)	(−182.03)	(−189.80)

[a] Values outside the parentheses are B3LYP/6-31+G**//6-31G* results; values inside the parentheses are B3LYP/6-31G* results. [b] 1 hartree = 627.51 kcal/mol

ligands. To assess the relative binding ability of the six exogenous ligands with catalytic zinc ion, five ligand-exchange virtual reactions were designed as presented by reactions 1−5.

model **1** (C2) + CH_3S^- (L1) =
$\qquad$ model **2** (C1) + water (L2) (rxn 1)

model **1** (C2) + hydroxamate (L1) =
$\qquad$ model **3** (C1) + water (L2) (rxn 2)

model **1** (C2) + formylhydroxylamine (L1) =
$\qquad$ model **4** (C1) + water (L2) (rxn 3)

model **1** (C2) + hypophosphite (L1) =
$\qquad$ model **5** (C1) + water (L2) (rxn 4)

model **1** (C2) + acetate (L1) =
$\qquad$ model **6** (C1) + water (L2) (rxn 5)

The thermodynamic parameters of the internal energy change (ΔE_t), thermal energy change (ΔE_{therm}), entropy change (ΔS), and free energy change (ΔG) of the ligand-exchange reactions 1−5 were calculated employing equations 1−5. The calculation results are also listed in Table 3.

$$\Delta E_t = E_t(C1) + E_t(L2) - E_t(C2) - E_t(L1) \qquad (1)$$
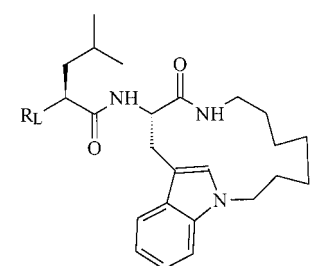
$$\Delta E_{therm} = E_{therm}(C1) + E_{therm}(L2) - E_{therm}(C2) - E_{therm}(L1) \qquad (2)$$

$$\Delta S = S(C1) + S(L2) - S(C2) - S(L1) \qquad (3)$$

$$\Delta H = \Delta E_t + \Delta E_{therm} + \Delta(PV) \qquad (\Delta(PV) = 0) \quad (4)$$

$$\Delta G = \Delta H - T\Delta S \qquad (5)$$

Quantum Chemistry Study on the Interaction

J. Phys. Chem. B, Vol. 106, No. 17, 2002 **4557**

TABLE 4: The Structures and Inhibitory Constants of Indolactam-Based Inhibitors to Matrilysin (K_i) and HFC (K'_i) and the Calculated Free Energy Changes of Reactions 1−5

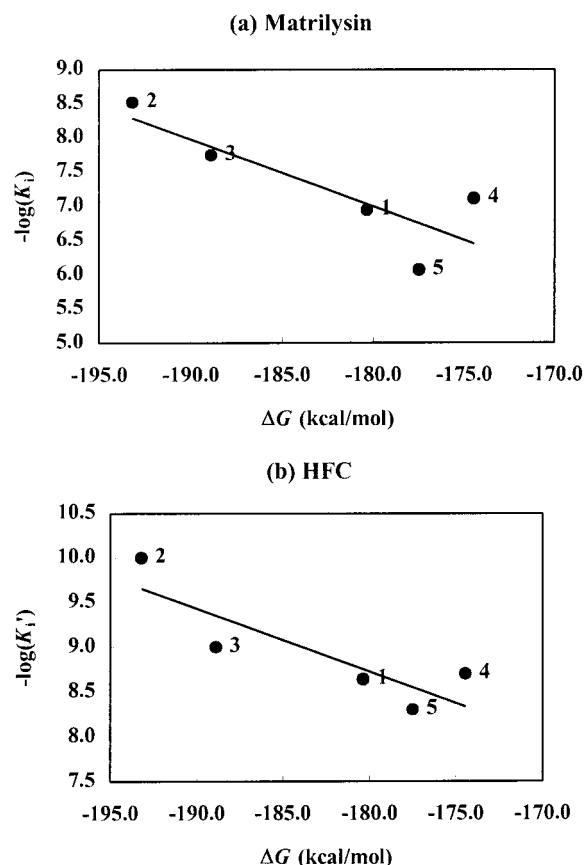| No	R_L	K_i (nM)	-logK_i	K'_i (nM)	-logK'_i	ΔG (kcal/mol)[a]
1	HS	114	6.94	2.3	8.64	-180.34
2	HOHN—C(O)	3	8.52	0.1	10.0	-193.19
3	H—C(O)—N(OH)	18	7.74	1.0	9.0	-188.89
4	quinoline-S-CH2-P(O)(OH)	78	7.11	2	8.70	-174.45
5	HO—C(O)	850	6.07	5	8.30	-177.48

[a] B3LYP/6-31+G**//6-31G* calculation results.

The free energy changes (ΔG) for the ligand-exchange reactions reflect the binding ability of the exogenous ligands with Zn(II) relative to water molecule. With the decrease of this value, the corresponding ligand's binding ability to zinc ion increases. As shown in Table 3, the binding ability of the various ligands to zinc ion is in the descent order hydroxamate > formylhydroxylamine > CH_3S^- > acetate > hypophosphite. This order can be well explained by the structural and charge characteristics of the complexes discussed above. Although hydroxamate, formylhydroxylamine, acetate and hypophosphite all coordinate with Zn(II) by using two oxygen atoms, the optimized structures of models **1−6** (Figure 2) by B3LYP/6-31G* indicate that hypophosphite and acetate bind to the zinc ion with one O−Zn(II) coordination bond and an O···Zn(II) electrostatic interaction (partial coordination bond), forming a tensional four-member ring (O2−P18(C18)−O19 with Zn(II)), while the other two bidentate ZBGs coordinate with Zn(II) forming a strainless five-member ring (O2−C18−N20−O19 with Zn(II)) (Figure 2 and Table 1). The lower tension is probably the reason hydroxamate and formylhydroxylamine are more active than acetate and hypophosphite as ZBGs. CH_3S^- coordinates to the zinc ion with a single atom; however, the coordinating ability of the S atom is more powerful than that of the oxygen atom, which makes CH_3S^- a good zinc binding group. The conclusion is also proved by atomic charge analyses. As shown in Table 2, the atomic charge on the zinc ion in model **2** is especially low compared with other oxygen-coordination models, and the group negative charge transferring from CH_3S^- to the zinc ion is remarkable. This indicates that the positive charge of Zn(II) may be delocalized by CH_3S^-, which stabilizes the structure of model **2**. Therefore, we can conclude that the structural and atomic charge parameters of models **2−6** are in agreement with their binding affinities with Zn(II).

A New Strategy for ZBG Design. One of the key problems in the design of MMP inhibitors is how to find the best ZBG

for competing with substrate to coordinate the zinc ion. The binding affinity of ZBGs of MMP inhibitors with Zn(II) plays an important role in the activity of the inhibitors; if the remaining parts of the inhibitors are the same or similar, the activity may correlate with the binding affinity of the ZBGs with Zn(II).[27] As shown above, quantum chemistry calculations can quantitatively describe the binding ability of exogenous ligands with the catalytic zinc ion in matrix metalloproteinases. This also gives a clue to the design of new ZBGs for MMP inhibitors for increasing the activity. By selecting a suitable complex model, it is possible to use our strategy, design the virtual reactions, optimize the structures, and calculate the relative binding ability of the designed ZBGs, for predicting the activity of new synthesized MMP inhibitors; those potential inhibitors encoding a ZBG that would exhibit stronger relative binding free energy to Zn(II) than the old ZBG using this paradigm would therefore be expected to have greater efficacy toward MMPs.

To verify our new strategy for ZBG design, a series of MMP inhibitors synthesized by Castelhano et al.[27] were selected as our test molecules. Their structures and in vitro inhibitory constants targeting two MMPs, matrilysin (K_i) and human fibroblast collagenase (HFC) (K'_i), are listed in Table 4. These inhibitors possess different ZBGs, while the rest of the inhibitor structure is almost "constant". As it has been indicated above, their inhibitory activities should correlate with the binding ability of their ZBGs toward Zn(II).

Because the relative binding affinities (ΔG's) of the five ZBGs encoded in the inhibitors in Table 4 have been obtained (Table 3), employing partial least-squares (PLS) analysis, we calculated regression equations for the experimental binding affinities, $-\log K_i$'s and $-\log K'_i$'s, using the calculated relative binding affinity, ΔG, as descriptor variable. B3LYP/6-31G* calculated results of ΔG have a moderate correlation with $-\log K_i$'s and $-\log K'_i$'s, $r = 0.724$ and 0.774, respectively. However, ΔG's derived from the B3LYP/6-31+G**//6-31G* single-point

4558 *J. Phys. Chem. B, Vol. 106, No. 17, 2002*

Cheng et al.

(a) Matrilysin

(b) HFC

Figure 3. The correlation between the inhibitory activities of the indolactam-based inhibitors to matrilysin ($-\log K_i$) (a) and HFC ($-\log K'_i$)[27] (b) and the calculated free energy changes (ΔG) of reactions 1−5.

energy calculations correlate well with the experimental binding affinities, $r = 0.843$ and 0.854, respectively (eqs 6 and 7), and the relationships are also shown graphically in Figure 3. This illustrates the importance of diffused orbitals for the energy calculation of anionic species.

$$\log K_i = -0.0979\Delta G - 10.622$$

$$s = 0.569, \quad r = 0.843, \quad F = 7.367 \tag{6}$$

$$\log K'_i = -0.0704\Delta G - 3.941$$

$$s = 0.0389, \quad r = 0.854, \quad F = 8.224 \tag{7}$$

As indicated in Figure 3, the binding affinities of inhibitors **1−3** and **5** have a much better correlation with the calculated free energies. The correlation coefficients increased to 0.969 and 0.939, respectively, for $-\log K_i$'s and $-\log K'_i$'s if inhibitor **4** was excluded in the regression (eqs 8 and 9). The departure of inhibitor **4** from the linear relationship is due to its ZBG structure. Different from the other inhibitors in Table 4, the ZBG encoded in inhibitor **4** is not a purely hypophosphite; it is a quinoline derivative of hypophosphite. The additional quinoline may bind with the S′₁ site of MMPs, which enhances the binding affinity of the inhibitor. Taking out the quinoline−MMP interaction may make inhibitor **4** go back to the linear relationships of ΔG with $-\log K_i$'s and $-\log K'_i$'s. The good correlations between the binding constants and the calculated free energy changes prove the reasonability and reliability of our strategy for probing the interaction mode of zinc ion with

exogenous ligands and show the possibility that our computational paradigm may be extended to ZBG design.

$$\log K_i = -0.141\Delta G - 18.771$$

$$s = 0.256, \quad r = 0.969, \quad F = 48.625 \tag{8}$$

$$\log K'_i = -0.0943\Delta G - 8.455$$

$$s = 0.310, \quad r = 0.939, \quad F = 14.848 \tag{9}$$

Conclusions

Six Zn(II) complexes, ZnX_3Y (where X = imidazole and Y = water, CH_3S^-, hydroxamate, formylhydroxylamine, hypophosphite, and acetate), have been calculated by a quantum chemistry method. The calculation results gave a detailed picture of zinc−ligand interaction and its influence on the activities of MMP inhibitors. In summary, our calculation allows for the following conclusions:

(1) The exogenous ligands may coordinate with the zinc ion in multiple fashions. Among these six exogenous ligands, water and CH_3S^- coordinate with zinc ion in a monodentate model to form four-coordination complexes, hydroxamate and formylhydroxylamine bond to Zn(II) in a bidentate model, and carboxylate and hypophosphite coordinate to Zn(II) in a way between monodentate and bidentate models.

(2) The zinc−ligand interaction may have obvious influence on the activities of MMP inhibitors. The water molecule can be activated after coordinating with the zinc ion of MMPs and thus acts as an effective nucleophile to attack and degrade the substrate of MMPs. As to hydroxamate, formylhydroxylamine, CH_3S^-, and hypophosphite, their binding abilities to the zinc ion are strong. These exogenous ligands can compete with substrate to coordinate zinc ion in MMPs, and therefore, they are all regarded as good ZBGs of MMP inhibitors.

(3) Our quantum chemistry calculation strategy is an effective and reliable method to probe the interaction between zinc ion and exogenous ligands. The optimized structures of these complexes are in agreement with the X-ray data in the Cambridge Structural Database and the PDB. Moreover, the geometric parameters of these complexes and the charge transfers between the exogenous ligands and the zicn ion characterize well the binding ability of these ligands with the zinc ion. This was also demonstrated by the relative binding free energy derived from the DFT computational results. The inhibitory activities of the MMP inhibitors containing the same substituents and different ZBGs correlate well with the relative binding free energies produced by the DFT calculation. This gives a possible good strategy for predicting the inhibitory activity of newly designed ZBGs. Those potential inhibitors that would exhibit strong binding ability of ZBGs to zinc ion using this paradigm would therefore be expected to have greater inhibitory activity.

Network Information Center, Chinese Academy of Sciences, Beijing, P. R. China.

References and Notes

(1) Matrisian, L. M. *Trends Genet.* **1990**, *6*, 121−125.

(2) Woessner, J. F., Jr. *FASEB J.* **1991**, *5*, 2145−2154.

(3) Cawston, T. E. *Pharmacol. Ther.* **1996**, *70*, 163−182.

(4) Yong, V. W.; Krekoski, C. A.; Forsyth, P. A.; Bell, R.; Edwards, D. R. *Trends Neurosci.* **1998**, *21*, 75−80.

(5) Wojtowicz-Praga, S. M.; Dickson, R. B.; Hawkins, M. J. *Invest. New Drugs* **1997**, *15*, 61−75.

(6) Talbot, D. C.; Brown, P. D. *Eur. J. Cancer* **1996**, *32A*, 2528−2533.

(7) Lovejoy, B.; Hassell, A. M.; Luther, M. A.; Weigl, D.; Jordan, S. R. *Biochemistry* **1994**, *33*, 8207−8217.

(8) Babine, R. E.; Bender, S. L. *Chem. Rev.* **1997**, *97*, 1359−1472.

(9) Morgunova, E.; Tuuttila, A.; Bergmann, U.; Isupov, M.; Lindqvist, Y.; Schneider, G.; Tryggvason, K. *Science* **1999**, *284*, 1667−1670.

(10) Wade, R. C. *Structure* **1997**, *5*, 1139.

(11) Kuntz, I. D. *Science* **1992**, *257*, 1078.

(12) Amzel, L. M. *Curr. Opin. Biotechnol.* **1998**, *9*, 366−369.

(13) Kuntz, I. D.; Blaney, J. M.; Oately, S. J. *J. Mol. Biol.* **1982**, *161*, 269.

(14) Shoichet, B. K.; Bodian, D. L.; Kuntz, I. D. *J. Comput. Chem.* **1992**, *13*, 505.

(15) Roothan, C. C. *J. Rev. Mod. Phys.* **1951**, *23*, 69.

(16) Hohenberg, P.; Kohn, W. *Phys. Rev.* **1964**, *136*, B864.

(17) Kleifeld, O.; Van Den Steen, P. E.; Frenkel, A.; Cheng, F.; Jiang, H. L.; Opdenakker, G.; Sagi, I. *J. Biol. Chem.* **2000**, *275*, 34335−34343.

(18) Becke, A. D. *J. Chem. Phys.* **1993**, *98*, 5648.

(19) Ryde, U. *Biophys. J.* **1999**, *77*, 2777−2787.

(20) Head-Gordon, M.; Head-Gordon, T. *Chem. Phys. Lett.* **1994**, *220*, 122.

(21) Frisch, M. J.; Trucks, G. W.; Schlegel, H. B.; Scuseria, G. E.; Robb, M. A.; Cheeseman, J. R.; Zakrzewski, V. G.; Montgomery, J. A., Jr.; Stratmann, R. E.; Burant, J. C.; Dapprich, S.; Millam, J. M.; Daniels, A. D.; Kudin, K. N.; Strain, M. C.; Farkas, O.; Tomasi, J.; Barone, V.; Cossi, M.; Cammi, R.; Mennucci, B.; Pomelli, C.; Adamo, C.; Clifford, S.; Ochterski, J.; Petersson, G. A.; Ayala, P. Y.; Cui, Q.; Morokuma, K.; Malick, D. K.; Rabuck, A. D.; Raghavachari, K.; Foresman, J. B.; Cioslowski, J.; Ortiz, J. V.; Stefanov, B. B.; Liu, G.; Liashenko, A.; Piskorz, P.; Komaromi, I.; Gomperts, R.; Martin, R. L.; Fox, D. J.; Keith, T.; Al-Laham, M. A.; Peng, C. Y.; Nanayakkara, A.; Gonzalez, C.; Challacombe, M.; Gill, P. M. W.; Johnson, B. G.; Chen, W.; Wong, M. W.; Andres, J. L.; Head-Gordon, M.; Replogle, E. S.; Pople, J. A. *Gaussian 98*, revision A.7; Gaussian, Inc.: Pittsburgh, PA, 1998.

(22) *Sybyl*, 6.6 ed.; Tripos Inc.: St. Louis, MO.

(23) Bernstein, F. C.; Koetzle, T. F.; Williams, G. J.; Meyer, E. E., Jr.; Brice, M. D.; Rodgers, J. R.; Kennard, O.; Shimanouchi, T.; Tasumi, M. *J. Mol. Biol.* **1977**, *112*, 535−542.

(24) Whittaker, M.; Floyd, C. D.; Brown, P.; Gearing, A. J. H. *Chem. Rev.* **1999**, *99*, 2735−2775.

(25) Alberts, I. L.; Nadassy, K.; Wodak, S. J. *Protein Sci.* **1998**, *7*, 1700−1716.

(26) Clementi, E.; Corongiu, G.; Jonsson, B.; Romano, S. *FEBS Lett.* **1979**, *100*, 313−317.

(27) Castelhano, A. L.; Billedeau, R.; Dewdney, N.; Donnelly, S.; Horne, S.; Kurz, L. J.; Liak, T. J.; Martin, R.; Uppington, R.; Yuan, Z.; Krantz, A. *Bioorg. Med. Chem. Lett.* **1995**, *5*, 1415−1420.